

1 **Towards optimal sampling design for spatial capture-** 2 **recapture**

3 Gates Dupont¹, J. Andrew Royle², Muhammad Ali Nawaz^{3,4}, Chris Sutherland^{1*}

4 ¹ University of Massachusetts–Amherst, MA, USA

5 ² U.S. Geological Survey, Laurel, MD, USA

6 ³ Department of Animal Sciences, Quaid-i-Azam University, 44000, Islamabad,

7 Pakistan

8 ⁴ Snow Leopard Trust, Seattle, WA, USA

9 * Corresponding author: csutherland@umass.edu

10 **Abstract**

11 Spatial capture-recapture (SCR) has emerged as the industry standard for
12 analyzing observational data to estimate population size by leveraging information from
13 spatial locations of repeat encounters of individuals. The resulting precision of density
14 estimates depends fundamentally on the number and spatial configuration of traps.
15 Despite this knowledge, existing sampling design recommendations are heuristic and
16 their performance remains untested for most practical applications - i.e.,
17 spatially-structured and logistically challenging landscapes. To address this issue, we
18 propose a genetic algorithm that minimizes any sensible, criteria-based objective
19 function to produce near-optimal sampling designs. To motivate the idea of optimality,
20 we compare the performance of designs optimized using two model-based criteria
21 related to the probability of capture. We use simulation to show that these designs
22 out-perform those based on existing recommendations in terms of bias, precision, and
23 accuracy in the estimation of population size. Our approach allows conservation
24 practitioners and researchers to generate customized sampling designs that can improve
25 monitoring of wildlife populations.

26 **Keywords**— SCR, spatial capture-recapture, spatially-explicit capture-recapture,
27 camera traps, density, optimal design, sampling design, spatial sampling, trap spacing

28 **Introduction**

29 In order to conserve wildlife, managers must obtain reliable estimates of density
30 (Williams et al., 2002) which has driven the development of data collection and estimation
31 methods, especially those that can account for imperfect detection. Capture-recapture (CR),
32 and more recently, spatial capture-recapture (SCR: Royle et al., 2014) methods were
33 developed specifically for this purpose and are now routinely applied in ecological research.
34 Concurrently, SCR methods estimate detection, space use, and density by analyzing

35 individual encounter histories while explicitly incorporating auxiliary information from the
36 spatial organization of encounters (Efford, 2004; Royle et al., 2014). Despite widespread
37 adoption and rapid method development, recommendations about spatial sampling design
38 have received relatively little attention and are arguably heuristic.

39 The effects of sampling design have been investigated for both CR (Dillon and Kelly
40 2007; Bondrup-Nielsen 1983; Gardner et al. 2010) and SCR methods (discussed in the next
41 paragraph). While CR methods aim to balance the number of captures and the number of
42 recaptures, SCR requires a third consideration, the number of spatial recaptures, i.e., the
43 number of times individuals are observed at multiple locations. The ability to reliably
44 estimate these quantities is directly related to the quality of the data collected: the number of
45 captured individuals n is the sample size; the number of recaptures is directly related to the
46 baseline detection probability, g_0 ; and the number and spatial distribution of recaptures are
47 directly related to the spatial scale parameter, σ . Therefore, improving sampling design has
48 great potential to increase the quality of the data and the precision of estimates.

49 Several simulation studies evaluating SCR designs have shown that the model is robust
50 to the spatial configuration of traps, as long as some minimum requirements are met: the
51 trap spacing must not be too large relative to individual space use in order to accurately
52 estimate σ , but the array must not be too small such that too few individuals are exposed to
53 capture (Sollmann et al., 2012; Sun et al., 2014; Wilton et al., 2014; Efford and Boulanger,
54 2019). Repeated illustrations of this trade-off have lead to the recommendation that trap
55 spacing should be approximately two times σ , which maximizes accuracy and minimizes bias
56 of abundance estimates (Sollmann et al., 2012; Efford and Fewster, 2013; Royle et al., 2014;
57 Efford and Boulanger, 2019). While most research has focused on complete, uniform grids,
58 there is evidence also that clustered designs can outperform uniform designs, offering better
59 capability to sample larger areas (Efford and Fewster, 2013; Sun et al., 2014), with further
60 evidence suggesting that this is particularly useful for heterogeneously distributed populations
61 (Efford and Fewster, 2013; Wilton et al., 2014). In summary, the idea of optimal sampling

62 design for SCR remains poorly understood in general. In particular, it is unclear whether
63 existing design heuristics hold for spatially-varying density patterns, or in highly-structured
64 landscapes where recommended regular trapping arrays can not be accommodated.

65 Sampling design for SCR can be conceived as a problem of selecting a subset of all
66 possible trap locations that maximizes some SCR-relevant objective function. Here we
67 develop an analytical framework that directly addresses this challenge. Our approach
68 generates an optimal sampling design with respect to some appropriate objective function and
69 information about available resources (traps), a set of possible trap locations, and information
70 about SCR model parameters. To motivate the idea of optimality, we compare the
71 performance of designs optimized using two model-based criteria related to current thinking
72 about the relationship between data quality and estimator bias and precision and leverage the
73 encounter process. We use simulation to demonstrate that optimal designs generated using
74 our framework perform well, producing unbiased and precise estimates of abundance. Further,
75 we show that these designs are robust to the geometry of the landscape, deviations from
76 uniform spatial distribution of individuals, and variation in spatial coverage of the trapping
77 array. Our proposed framework is flexible and can be generalized to any species of interest
78 and to any landscape.

79 **Methods**

80 **The standard SCR model**

81 Typically, SCR models have two model components: a spatial model of abundance
82 describing the distribution of individuals characterized by the center of their home range
83 (hereby referred to as an activity center), and a spatial model of detection that relates
84 encounter rates to the distance between the activity center and a trap (e.g., a camera trap
85 located at a point in space) at which the individual was captured. The most basic form
86 assumes a uniform prior for the distribution of activity centers, s_i :

$$s_i \sim \text{Uniform}(\mathcal{S}),$$

87 where \mathcal{S} , referred to as the state-space, describes all possible locations of individual activity
88 centers within the study area. To facilitate analysis, \mathcal{S} is discretized as a uniform grid of
89 points representing the centroids of equal-sized pixels. The total population size within the
90 region, N , is exposed to capture resulting in n observed individuals and hence $n_0 = N - n$
91 unobserved individuals.

92 While several formulations of the encounter model exist, we use, without loss of
93 generality, a half-normal encounter model that describes encounter probability as a decreasing
94 function of distance from an individual's activity center s_i :

$$p_{ijk} = g_0 \times \exp(-d(s_i, x_j)^2 / (2\sigma^2)), \quad (1)$$

95 where p_{ijk} is the probability of detecting an individual i with activity center s_i at trap j
96 during sampling occasion k ; $d(s_i, x_j)$ is the distance between the activity center s_i and the
97 trap x_j , and g_0 and σ are parameters to be estimated. In biological terms, an individual is
98 more likely to be captured at a trap that is closer to its activity center such that σ serves as a
99 proxy for animal space use, relying on spatial recaptures (m) for its estimation.

100 Model-based objective functions

101 From Equation 1, we can use values of g_0 and σ (e.g., from the literature or estimates
102 from a pilot study), to compute the probability that an individual with an activity center s_i
103 is detected in *any* trap in an array \mathcal{X} , which we denote as \bar{p} :

$$\bar{p}(s_i, \mathcal{X}) = 1 - \prod_{j=1}^J 1 - p(s_i, x_j).$$

104 The corresponding marginal probability of not being encountered is thus: $\bar{p}_0(s_i, \mathcal{X}) = 1 -$
105 $\bar{p}(s_i, \mathcal{X})$. Taking the average over all G activity center locations in the landscape \mathcal{S} , we can
106 compute the marginal probability of encounter:

$$\bar{p}(\mathcal{X}) = \frac{1}{G} \sum_s \bar{p}(s_i, \mathcal{X}).$$

107 We can also compute the probability of being captured in exactly one trap:

$$\bar{p}_1(s_i, \mathcal{X}) = \bar{p}_0(s_i, \mathcal{X}) \sum_{j=1}^J \frac{p(s_i, x_j)}{1 - p(s_i, x_j)}.$$

108 Finally, the marginal probability of being encountered at more than one trap, i.e., of a spatial
109 recapture is:

$$\bar{p}_m(\mathcal{X}) = \frac{1}{G} \sum_s 1 - \bar{p}_0(s_i, \mathcal{X}) - \bar{p}_1(s_i, \mathcal{X}).$$

110 Given that the precision of density estimates in spatial capture-recapture depends on
111 two aspects of the data – the total number of individuals captured, n , and the number of
112 spatial recaptures, m (Efford and Boulanger, 2019; Royle et al., 2014) – the quantities above
113 represent logical criteria for generating optimal SCR designs (Royle et al. 2014, Chapter 10).
114 Hence, we suggest two design criteria to be minimized: $Q_{\bar{p}} = -\bar{p}(\mathcal{X})$, and $Q_{\bar{p}_m} = -\bar{p}_m(\mathcal{X})$.
115 Importantly, if approximate values of the SCR parameters, g_0 and σ , are available, these
116 objective functions can be evaluated for any number and configuration of traps, thus
117 providing a metric for identifying ‘optimal’ SCR designs.

118 Optimization method

119 To identify the optimal subset of locations that minimize $Q_{\bar{p}}$ or $Q_{\bar{p}_m}$, we used a genetic
120 algorithm implemented by the function `scrdesignGA()` in the `oSCR` package (Sutherland
121 et al., 2019). This function is a wrapper of the function `kofnGA()` from its namesake package,
122 `kofnGA` (Wolters, 2015) with additional arguments to extend the function’s utility for
123 generating SCR sampling designs. The *k-of-n* problem is an appropriate application as it
124 describes concisely the challenge of the SCR sampling design problem where some number of
125 traps, k , must be placed in a landscape comprised of n possible locations and configured to
126 optimize some objective function, which presented here is one of two SCR-specific criteria.

127 The criteria $Q_{\bar{p}}$ is a space-filling objective function that spreads traps across the
128 landscape and maximizes exposure of individuals to detection (Appendix 1). Thus,
129 minimizing this quantity should maximize the expected sample size n . In contrast, $Q_{\bar{p}_m}$
130 prioritises the exposure of individuals to more than one trap, resulting in more compact or

131 clustered configurations relative to those produced by minimizing $Q_{\bar{p}}$. Minimizing $Q_{\bar{p}_m}$ should
132 maximize the number of spatial recaptures m .

133 Design constraints

134 Our primary motivation is to evaluate, using simulation, the performance of SCR
135 designs produced by our proposed framework, employing the two design criteria described
136 above: $Q_{\bar{p}}$ and $Q_{\bar{p}_m}$. In addition, and where possible, we also evaluate the regularly-spaced,
137 2σ grid design, as it represents current design recommendations (Sollmann et al., 2012; Royle
138 et al., 2014; Efford and Boulanger, 2019). For our measures of performance, we focus on
139 relative bias, precision, and accuracy of estimates of total abundance. Beyond standard
140 testing scenarios, we are interested in evaluating the performance of these designs under a
141 range of biologically-realistic scenarios in an attempt to develop a more general understanding
142 of how performance varies as a function of the following design constraints: *geometry*, defined
143 as the shape of the study area and ease at which a regular square trapping grid can be
144 deployed; *density pattern*, defined as the nature of departure from uniform distribution of
145 individuals; and *effort*, defined as the number of traps available for the design.

146 **Geometry** – As has been typical in studies investigating SCR sampling designs, we
147 begin using a square study area with complete accessibility and which lends itself to uniform
148 grids of traps (the *regular area*, Figure 1). To replicate the design challenges posed when
149 generating real-world designs, we also consider an *irregular area* (Figure 1). For this, we use
150 one of the study areas that motivated this work: a large area in Northern Pakistan (3865
151 km^2) that is the focus of a snow leopard (*Panthera uncia*) camera trapping study, but that
152 has several logistical challenges that determine accessibility (i.e., remoteness, altitude, and
153 slope). To define the complete region of the state-space, we used a 3σ buffer around the
154 trapping extent. The regular area is represented by 24 x 24 landscape with a resolution of 0.5
155 units, the irregular study area is represented by 89.85 x 133.04 landscape with a resolution of
156 1.73 units, for a total of 2304 cells in each of the geometries (Figure 1). While these two
157 state-spaces differ in absolute terms, we insured comparability in relative terms by the

158 definition of area-specific sigma (see below).

159 **Density pattern** – Existing investigations of SCR sampling designs typically assume a
160 homogeneous distribution of individuals (but see Efford and Fewster, 2013). Here we formally
161 test the adequacy of designs under specific violations of this assumption. As such, we consider
162 three classes of spatial density patterns for the state-space: one uniform and two
163 spatially-varying. To generate non-uniform density patterns, we simulated landscapes with
164 spatial dependence by employing a parametric Gaussian random field model that allows for
165 specification of the degree and range of spatial autocorrelation. Gaussian random fields were
166 generated using the R package, NLMR (Sciaini et al., 2018). The values of the simulated
167 landscape were scaled from 0 to 1 and individual activity centers distributed according to the
168 following cell probabilities:

$$\pi_i = \frac{e^{\beta_1 * X_i}}{\sum e^{\beta_1 * X_i}}, \quad (2)$$

169 where X_i is the scaled landscape value at pixel i and β_1 is defined as 1.2 to represent a weak
170 but apparent density pattern. The two classes of non-uniform density patterns (generated
171 using the Gaussian random fields model) differ in the scale of spatial autocorrelation. For
172 consistency, we defined this distance in relative terms to the length of the longest side of the
173 state-space: 6% for a *weak* density pattern or 100% for a *strong* density pattern (see Figure 1
174 for a single realization of the density patterns). Weak spatial autocorrelation produces a
175 patchy landscape, while strong spatial autocorrelation produces a landscape with a more
176 contiguous gradient between area edges. Using these three density patterns allows us to
177 evaluate designs through a full range of biological realism, with uniform and strong density
178 patterns representing the polar ends of reality, and the patchy landscape representing the
179 most realistic sampling scenario.

180 Design generation

181 Designs were generated using fixed values of g_0 and σ (see below), a set of potential
182 trap locations, and the number of traps that are available to deploy. It is assumed that the

183 user would have a good sense of the parameter values for the focal species, that they would
184 be able to produce a set of all potential sampling points, and would have some idea of
185 resources (traps) available. Only geometry and effort affect the generation of optimal designs.
186 For the regular area, we generated $Q_{\bar{p}}$ and $Q_{\bar{p}_m}$ designs for each of the three levels of effort
187 where there was no restriction on where traps could be placed. In addition, we generated a
188 regular 2σ design for comparison. For the irregular area in the mountains of Pakistan, we
189 generated $Q_{\bar{p}}$ and $Q_{\bar{p}_m}$ designs at each of the three levels of effort (Figure 2). In this case,
190 areas that were too remote, too high altitude, or too steep to be accessed were removed from
191 the set of potential trap locations. Mirroring real design challenges faced by managers, it was
192 not practical to generate a 2σ grid for the irregular area, and therefore it is not included.
193 This full scenario analysis resulted in a total of 15 designs; 9 designs for the regular area
194 (three levels of effort for each of the $Q_{\bar{p}}$, $Q_{\bar{p}_m}$, and 2σ criteria), and 6 designs for the irregular
195 area (three levels of effort for the $Q_{\bar{p}}$ and $Q_{\bar{p}_m}$ criteria).

196 **Evaluation by simulation**

197 We exposed a population of $N = 300$ individuals to sampling via each of the 15 designs
198 described above. We simulated encounter histories under the binomial model above (Equation
199 1), assuming camera traps (proximity detectors), with $g_0 = 0.2$, $k = 5$, and area-specific
200 space-use parameters $\sigma_{reg} = 0.80$ and $\sigma_{irreg} = 2.59$. Because the two geometries differ in the
201 relative size of their spatial units, area-specific σ values were chosen such that the number of
202 home ranges required to fill the areas and achieve an equal density was equivalent. We
203 simulated individuals according to the three density patterns described above (Equation 2),
204 resulting in a total of 45 scenarios of interest (three density patterns for each of the 15
205 designs, see Appendix 2 for summary table).

206 For each scenario, we simulated 300 realizations of activity centers. Covariate surfaces
207 were generated randomly using the same seed, again resulting in variation among simulations
208 but consistency across scenarios. In some cases, the realization of activity centers did not
209 provide at least one spatial recapture; we recorded the number of these *failure* events and

210 generated a new realization of activity centers until a single spatial recapture was obtained in
211 order to proceed with model fitting. This only occurred for $Q_{\bar{p}}$ designs with minimum effort,
212 and for less than 5% of the simulations.

213 We analyzed the resulting encounter history data using a null SCR model (d).
214 Additionally, for scenarios involving non-uniform density patterns, we used the data
215 generating landscape values as a covariate in a density-varying model (d_s). This allowed us to
216 test if accounting for the landscape would improve bias and precision in parameter estimates.
217 For each simulation, and each model, we retained estimates of g_0 , σ , and \hat{N} .

218 Across the various designs, we compared estimates of model parameters to the
219 data-generating values in terms of bias, precision, and accuracy. We calculated the
220 discrepancy between estimates and true values relative to the true values for every simulation
221 and reported the mean of those values by scenario to represent bias (percent relative bias,
222 %RB). For precision, we calculated the coefficient of variation (CV) by scenario by taking the
223 standard deviation of parameter estimates relative to the mean of the estimates for that
224 scenario. Accuracy was evaluated by scenario using the root mean square error scaled to the
225 true value (scaled root mean square error, SRMSE). All simulations were conducted in R,
226 SCR models were fit using the package `oSCR` (Sutherland et al., 2019), and designs were
227 generated using the `scrdesignGA()` function also in `oSCR` (see Appendix 3 for an example).
228 Design generation and simulations were performed in R version 3.6.1 (R Core Team, 2019).

229 Results

230 Encouragingly, under the regular-area, homogeneous-density scenario, designs generated
231 using the optimal design algorithm perform as well as existing 2σ recommendations,
232 producing unbiased estimates of abundance for nearly all combinations of design and effort
233 (Figure 3, Table 1). In the case of the irregular geometry with uniform density, $Q_{\bar{p}_m}$ designs
234 perform well for all levels of effort, but performance of $Q_{\bar{p}}$ designs strongly declines as the
235 number of traps is reduced, which results in widely-spaced traps and consequently very few

236 spatial recaptures (Figure 3, Table 1, Appendix 4, Appendix 5, Appendix 6).

237 For scenarios from the regular study area with inhomogeneous density, all designs
238 produced unbiased estimates of abundance, generally. There is a slight bias ($\pm 5\%$)
239 introduced as the number of traps declines, even for the 2σ designs. However, this
240 phenomenon is less apparent in $Q_{\bar{p}_m}$ designs. In the irregular study area, design performance
241 is more dependent on the spatial structure of density. Once again, $Q_{\bar{p}_m}$ designs produced
242 unbiased estimates, but $Q_{\bar{p}}$ designs continue to perform poorly with fewer traps (Figure 3,
243 Table 1, Appendix 4, Appendix 5, Appendix 6).

244 Interestingly, explicitly including the landscape covariate governing spatial variation in
245 density (i.e., d_s rather than d .) does not appear to improve performance of the designs in any
246 scenario (Figure 3, Table 1), reinforcing the general opinion that SCR models are robust to
247 misspecification of the density model. In fact, fitting the data-generating model for the
248 inhomogeneous cases actually performs worse in low effort scenarios. This suggests that the
249 low numbers of traps do not adequately represent the variation in the landscape, and
250 therefore, the model is unable to estimate the underlying landscape effect (Figure 3, Table 1).

251 Precision and accuracy (Appendix 4 and Appendix 5, and Appendix 6, respectively)
252 generally follow the same patterns as for the bias. Design performance decreases with
253 decreasing effort for all designs across every scenario. In the regular study area with uniform
254 density, the 2σ and $Q_{\bar{p}_m}$ designs share similar levels of precision, while the $Q_{\bar{p}}$ design with
255 minimal effort is less precise in comparison, with this pattern being magnified in the irregular
256 area. Generally, there is a slight loss of precision in estimates across all designs, but less so for
257 $Q_{\bar{p}_m}$ designs, which maintain their relative equivalency to the standard recommendation,
258 including for the lowest level of effort (when considering comparison across geometries). In
259 scenarios with inhomogeneous density, only $Q_{\bar{p}}$ designs with minimum effort show precision
260 that is obviously reduced using the null model. However, the density-varying model once
261 again shows no noticeable improvement, and causes a decrease in precision for $Q_{\bar{p}_m}$ designs
262 with the fewest traps.

263 Overall, designs generated using our proposed framework showed comparable
264 performance to standard recommendations, and critically, these designs are robust to a
265 variety of constraints that include effort, density signal, and geometry.

266 Discussion

267 In this study, we develop a conceptual and analytical framework for generating optimal
268 designs for SCR studies. We suggested two intuitive and statistically-grounded design criteria
269 that can be optimized to produce candidate designs. We demonstrate that designs generated
270 using our framework perform as well as designs based on existing design heuristics, and that
271 the generality of our approach means it can be applied to any species or landscape according
272 to logistics and available resources.

273 It is worth noting that the designs produced using this framework can be considered
274 approximate in terms of specific location, and that the actual, finer-scale site-selection for
275 traps can be informed by knowledge of the species' biology and behavior (e.g., Fabiano et al.,
276 2020). Further, while we develop this framework with camera traps in mind, this method can
277 easily be applied to determine the general location of other non-invasive surveys, wherein the
278 selection of a sampling location instead activates some other form of sampling effort (see
279 Fuller et al. 2016; Sutherland et al. 2018). Importantly, the degree of sampling effort must be
280 maintained among all selected sampling locations.

281 The designs we created using model-based criteria exhibit two unique behaviors
282 (Appendix 1). The $Q_{\bar{p}}$ criteria generates space-filling designs to maximize the area covered
283 and thereby the expected sample size of unique individuals. As more traps are added, the
284 inner area becomes fully-saturated (such that it is insured that every possible home range will
285 contain at least one trap), and the criteria instead focuses on selecting external traps that
286 patrol the edge of the trapping extent in order to increase the probability of capture for
287 individuals outside of that area. However, despite the benefit of increasing the sample size (n
288 captured individuals), traps placed too distant from each other fail to generate important

289 spatial recaptures. This is precisely the issue that propagated failures for the $Q_{\bar{p}}$ design with
290 minimum effort.

291 In contrast, $Q_{\bar{p}_m}$ designs are space-restricting as a result of an inherent trade-off
292 between finding individuals to capture and having traps close together to insure captures at
293 more than one trap. With fewer traps, however, the effective sampling area is markedly
294 decreased (Figure 2), thereby reducing the sample size. This observation further motivated
295 our evaluations of the designs for inhomogeneous density, and is likely responsible for the
296 slight bias introduced in those scenarios, as well as the lower precision.

297 More generally, these designs support previous recommendations while also providing
298 new insights into sampling design for SCR. When full effort is possible in the regular area
299 geometry, the $Q_{\bar{p}}$ design fully saturates the trapping extent with some traps to spare in order
300 to meet its objective, while $Q_{\bar{p}_m}$ does not quite fill the trapping area (Figure 2, Appendix 1).
301 Interestingly, the 2σ design falls somewhere between these two extents, likely striking an
302 effective balance between the number of captures (as in $Q_{\bar{p}}$) against the number of spatial
303 recaptures (as in $Q_{\bar{p}_m}$), similar to the effect described by Efford and Boulanger (2019).
304 Despite these differences in spatial configuration, differences in design performance are mostly
305 negligible (Figure 3, Table 1, Appendix 4, Appendix 5, Appendix 6).

306 As shown by Sun et al. (2014), incorporating trap clustering into sampling designs can
307 be advantageous, as doing so allows for increased likelihood of spatial recaptures to facilitate
308 estimation of the spatial scale parameter, σ . However, the clustered designs proposed by Sun
309 et al. (2014) follow a regular pattern such that there are only a few levels of trap spacing,
310 whereas the designs we generated result in a wider distribution of distances between traps.
311 This shifts the importance away from a regular spatial structure of trap configuration to one
312 that is decidedly irregular in order to gain better resolution of movement distances for
313 estimating σ . This is especially useful knowledge and central to generating designs for
314 irregular study areas. Interestingly, this results in designs with smaller effective sampling
315 areas, suggesting that it might be better to reduce the total area covered by the design rather

316 than focus on completely covering the area (within reason). A major insight here is that
317 hierarchical clustering (the selection of approximately 2σ -spaced clusters of traps with further
318 reduced within-cluster spacing) emerges naturally from the $Q_{\bar{p}_m}$ criterion, effectively
319 formalizing the clustering heuristic proposed by Sun et al. (2014).

320 Our proposed criteria produced designs which perform well, yet there is scope for
321 improvement. With a decrease in effective sampling area, the introduction of bias and
322 imprecision in parameter estimates could be complicated further when the population being
323 sampled has a stronger degree of spatial structuring than we tested here. Designs sampling
324 only areas where individuals are concentrated will result in overestimates of population size
325 and density relative to the whole study area, while those sampling away from concentrated
326 areas will do just the opposite. This effect is particularly noticeable from the density-varying
327 model (d_s), which generally has relatively lower performance over the fully invariant model as
328 it is including information from nearby traps sampling a landscape that is intrinsically has
329 spatial auto-correlation. Advancing this framework to generate designs that explicitly account
330 for the spatial patterns in density as a function of a given landscape is clearly an area for
331 further development, especially if the inferential objective is to estimate density-landscape
332 relationships rather than total density or abundance.

333 Recently SCR sampling design for multi-species sampling has been considered, with
334 some discussion on how the distribution of trap spacing can allow for better estimates for
335 species with a variety of home range sizes (Rich et al., 2019). However, the design proposed
336 for this purpose lacks a reproducible framework that can be generalized to any biological
337 community. Alternatively, employing our framework for multi-species sampling could be a
338 straightforward approach to this problem, with important implications for the use of SCR to
339 be more easily applied for the study of biological populations. Again, a highly appealing
340 feature of our $Q_{\bar{p}_m}$ approach is the emergence of designs with much better distribution of trap
341 spacing than under regular designs such as 2σ grids.

342 We considered two criteria that are intuitive in the context of the performance trade off

343 of sample size (n) and spatial recaptures (m). While intuitive, alternative criteria surely exist.
344 For example, Efford and Boulanger 2019 propose an approximation of the variance of density
345 which is related to n and m , and therefore can easily be formulated as an objective function
346 to be optimized in the same way as $Q_{\bar{p}}$ and $Q_{\bar{p}_m}$. Indeed, the function `scrdesignGA()` is
347 designed such that any user-defined objective functions can be used. We hope that this
348 ability to simultaneously (and efficiently) generate and evaluate designs based on a variety of
349 design criteria will motivate further research on SCR study design.

350 Our results show that designs obtained under the our proposed criteria perform well
351 relative to design heuristic and can be obtained efficiently as solutions to an optimization
352 problem for arbitrary configurations of possible trapping locations and landscapes, unlike
353 standard recommendations based on 2σ and cluster designs. Both CR and SCR studies are
354 extremely expensive and require substantial effort to conduct, making it imperative that
355 managers are provided with a method to select detector placement before deployment, such
356 as what we have presented here. As a result, designs will produce a greater amount of
357 expected information and will lead to more accurate estimates of parameters that describe
358 biological populations of interest, which is critical to conservation efforts around the world.

359 Acknowledgements

360 This work received support from Panthera, the Pakistan Snow Leopard and Ecosystem
361 Protection Program, and the Snow Leopard Foundation. We thank the Sutherland Lab
362 Group, especially Patricia Levasseur, as well as Katherine Zeller and Daniel Linden, for
363 improving the manuscript. Any use of trade, product, or firm names is for descriptive
364 purposes only and does not imply endorsement by the U.S. Government.

365 **Author contributions:** CS, JAR, GD devised the study. CS and JAR wrote the functions
366 for design generation. GD conducted simulations. GD wrote the manuscript with
367 contributions from all authors.

368 **Data availability:** Code metadata and code are available in Appendix 7 and Appendix 8.

369 Literature cited

- 370 Bondrup-Nielsen, S. (1983). Density estimation as a function of live-trapping grid and home
371 range size. *Canadian Journal of Zoology*, 61(10):2361–2365.
- 372 Dillon, A. and Kelly, M. J. (2007). Ocelot *Leopardus pardalis* in Belize: the impact of trap
373 spacing and distance moved on density estimates. *Oryx*, 41(4):469–477.
- 374 Efford, M. (2004). Density estimation in live-trapping studies. *Oikos*, 106(3):598–610.
- 375 Efford, M. G. and Boulanger, J. (2019). Fast evaluation of study designs for spatially explicit
376 capture–recapture. *Methods in Ecology and Evolution*, 10(9):1529–1535.
- 377 Efford, M. G. and Fewster, R. M. (2013). Estimating population size by spatially explicit
378 capture-recapture. *Oikos*, 122(6):918–928.
- 379 Fabiano, E. C., Sutherland, C., Fuller, A. K., Nghikembua, M., Eizirik, E., and Marker, L.
380 (2020). Trends in cheetah (*Acinonyx jubatus*) density in north-central Namibia. *Population*
381 *Ecology*, pages 1438–390X.12045.
- 382 Fuller, A. K., Sutherland, C. S., Royle, J. A., and Hare, M. P. (2016). Estimating population
383 density and connectivity of American mink using spatial capture-recapture. *Ecological*
384 *Applications*, 26(4):1125–1135.
- 385 Gardner, B., Royle, J. A., Wegan, M. T., Rainbolt, R. E., and Curtis, P. D. (2010).
386 Estimating Black Bear Density Using DNA Data From Hair Snares. *Journal of Wildlife*
387 *Management*, 74(2):318–325.
- 388 R Core Team (2019). *R: A Language and Environment for Statistical Computing*. R
389 Foundation for Statistical Computing, Vienna, Austria.
- 390 Rich, L. N., Miller, D. A., Muñoz, D. J., Robinson, H. S., McNutt, J. W., and Kelly, M. J.
391 (2019). Sampling design and analytical advances allow for simultaneous density estimation

- 392 of seven sympatric carnivore species from camera trap data. *Biological Conservation*,
393 233:12–20.
- 394 Royle, J. A., Chandler, R. B., Sollmann, R., and Gardner, B. (2014). *Spatial Capture-*
395 *recapture*. AcademicPress/Elsevier.
- 396 Sciaini, M., Fritsch, M., Scherer, C., and Simpkins, C. E. (2018). Nlrm and landscapetools:
397 An integrated environment for simulating and modifying neutral landscape models in r.
398 *Methods in Ecology and Evolution*, 00:1–9.
- 399 Sollmann, R., Gardner, B., and Belant, J. L. (2012). How Does Spatial Study Design
400 Influence Density Estimates from Spatial Capture-Recapture Models? *PLoS ONE*,
401 7(4):e34575.
- 402 Sun, C. C., Fuller, A. K., and Royle, J. A. (2014). Trap Configuration and Spacing Influences
403 Parameter Estimates in Spatial Capture-Recapture Models. *PLoS ONE*, 9(2):e88025.
- 404 Sutherland, C., Fuller, A. K., Royle, J. A., Hare, M. P., and Madden, S. (2018). Large-scale
405 variation in density of an aquatic ecosystem indicator species. *Scientific Reports*, 8(1):8958.
- 406 Sutherland, C., Royle, J. A., and Linden, D. W. (2019). oSCR: a spatial capture–recapture R
407 package for inference about spatial ecological processes. *Ecography*, 42(9):1459–1469.
- 408 Williams, B. K., Nichols, J. D., and Conroy, M. J. (2002). *Analysis and Management of*
409 *Animal Populations : Modeling, Estimation, and Decision Making*. Academic Press, San
410 Diego, CA, first edition.
- 411 Wilton, C. M., Puckett, E. E., Beringer, J., Gardner, B., and Eggert, L. S. (2014). Trap
412 Array Configuration Influences Estimates and Precision of Black Bear Density and
413 Abundance. *PLoS ONE*, 9(10):111257.
- 414 Wolters, M. A. (2015). A Genetic Algorithm for Selection of Fixed-Size Subsets with
415 Application to Design Problems. *Journal of Statistical Software*, 68.

Table 1: Percent relative bias of baseline detection (g_0), space use (σ) and total abundance (EN) for each simulation scenario, varying: design criteria (*Design*), landscape shape (*Geometry*), the number of traps (*Effort*), and density patterns (*Density*). We present results from null ($d.$) and varying density (d_s) models.

Geometry	Effort	Density	Design	g_0		σ		EN		
				$d.$	d_s	$d.$	d_s	$d.$	d_s	
regular	49	uniform	2σ	2.52	-	-0.38	-	0.78	-	
			$Q_{\bar{p}_m}$	1.33	-	-0.19	-	1.76	-	
			$Q_{\bar{p}}$	0.82	-	-1.00	-	7.27	-	
		weak	2σ	3.16	3.16	-0.62	-0.61	-0.26	-0.05	
			$Q_{\bar{p}_m}$	0.08	0.08	0.06	0.11	0.99	1.99	
			$Q_{\bar{p}}$	-0.58	-0.58	0.20	0.25	5.70	5.75	
		strong	2σ	2.26	2.26	-0.47	-0.48	1.82	3.48	
			$Q_{\bar{p}_m}$	2.09	2.09	-0.47	-0.48	1.20	6.82	
			$Q_{\bar{p}}$	1.84	1.84	-0.75	-0.78	6.43	6.55	
	100	uniform	2σ	2.04	-	-0.69	-	0.58	-	
			$Q_{\bar{p}_m}$	-0.97	-	0.20	-	1.07	-	
			$Q_{\bar{p}}$	2.42	-	-0.61	-	0.90	-	
		weak	2σ	-0.13	-0.13	0.15	0.14	-0.34	-0.19	
			$Q_{\bar{p}_m}$	1.68	1.68	-0.77	-0.78	-0.24	0.34	
			$Q_{\bar{p}}$	0.61	0.61	-0.27	-0.29	0.95	0.98	
		strong	2σ	0.35	0.35	-0.3	-0.30	1.42	1.72	
			$Q_{\bar{p}_m}$	0.64	0.64	-0.04	-0.05	0.90	1.47	
			$Q_{\bar{p}}$	0.18	0.18	-0.93	-0.95	2.89	3.12	
	144	uniform	2σ	1.32	-	-0.25	-	0.27	-	
			$Q_{\bar{p}_m}$	0.93	-	-0.28	-	0.88	-	
			$Q_{\bar{p}}$	-1.06	-	0.28	-	1.53	-	
		weak	2σ	0.49	0.49	-0.33	-0.33	0.41	0.50	
			$Q_{\bar{p}_m}$	1.31	1.31	-0.47	-0.48	-0.39	-0.21	
			$Q_{\bar{p}}$	0.64	0.64	-0.24	-0.25	0.44	0.47	
strong		2σ	0.07	0.70	-0.25	-0.25	0.8	1.01		
		$Q_{\bar{p}_m}$	0.14	0.14	0.15	0.14	0.32	0.58		
		$Q_{\bar{p}}$	1.35	1.35	-0.31	-0.32	0.32	0.47		
irregular	49	uniform	$Q_{\bar{p}_m}$	1.78	-	-0.15	-	0.62	-	
			$Q_{\bar{p}}$	2.27	-	-1.84	-	8.34	-	
			$Q_{\bar{p}_m}$	1.15	1.15	-0.27	-0.22	0.07	2.74	
		weak	$Q_{\bar{p}}$	-1.51	-1.51	-1.11	-1.07	9.93	9.89	
			$Q_{\bar{p}_m}$	2.29	2.29	-1.03	-1.01	2.4	9.02	
			$Q_{\bar{p}}$	1.18	1.18	-0.27	-0.32	5.8	6.17	
		100	uniform	$Q_{\bar{p}_m}$	0.74	-	-0.18	-	0.83	-
				$Q_{\bar{p}}$	1.42	-	-0.77	-	2.11	-
				$Q_{\bar{p}_m}$	-0.09	-0.09	0.09	0.08	0.34	1.04
	weak		$Q_{\bar{p}}$	0.97	0.97	-0.48	-0.49	1.82	1.89	
			$Q_{\bar{p}_m}$	1.97	1.97	-0.56	-0.59	-0.44	1.34	
			$Q_{\bar{p}}$	1.07	1.07	-0.46	-0.49	0.93	1.4	
	144		uniform	$Q_{\bar{p}_m}$	0.53	-	0.00	-	0.75	-
				$Q_{\bar{p}}$	0.72	-	0.08	-	-0.27	-
				$Q_{\bar{p}_m}$	0.03	0.03	0.05	0.04	0.07	0.43
		weak	$Q_{\bar{p}}$	0.61	0.61	-0.20	-0.20	0.5	0.51	
			$Q_{\bar{p}_m}$	1.74	1.74	-0.55	-0.57	-0.22	0.69	
			$Q_{\bar{p}}$	-0.13	-0.13	0.21	0.19	0.33	0.66	

416 **Figure legends**

417 **Figure 1**

418 Simulation structure. Here we show all possible trap locations overlaid on the uniform
419 landscape for the regular (top) and irregular (bottom) study area geometries alongside a
420 single realization of two (weak: middle, strong: right) of the three (uniform not shown)
421 landscape covariates. For the regular geometry, we tested 9 designs each. For the irregular
422 geometry, we tested 6 designs each. This makes for a total of 45 scenarios.

423 **Figure 2**

424 Irregular study area with designs generated using our new framework with both SCR-
425 intuitive, model-based criteria ($Q_{\bar{p}}$ and $Q_{\bar{p}_m}$), under three levels of effort. 144 traps represents
426 the same number of traps as used to generate a full 2σ grid in a regular study area of the
427 same area. 100 traps is nearly two-thirds as many traps, and 49 is nearly one-third as many
428 traps. Each pixel of the state-space is colored according to the probability of capture, p , for
429 an individual with an activity centers at the centroid of the pixel.

430 **Figure 3**

431 Percent relative bias (%RB) of estimates of total abundance from the three tested
432 sampling designs under three levels of effort on three density surfaces within two geometries,
433 where estimates are the result of one of two SCR models: density invariant (d ., open shapes)
434 or density-varying (d_s , closed shapes). The three designs – 2σ , $Q_{\bar{p}}$, $Q_{\bar{p}_m}$ – are represented by
435 the three shapes: circles, triangles, and squares, respectively. To illustrate estimator accuracy,
436 vertical lines are 50% confidence intervals, noting that the 50% intervals are proportional to
437 95% intervals but offer a visual balance of bias and associated variance. The thick horizontal
438 line represents no bias in estimates, with the thin horizontal lines representing an allowable
439 amount of bias ($\pm 5\%$).

Figure 1

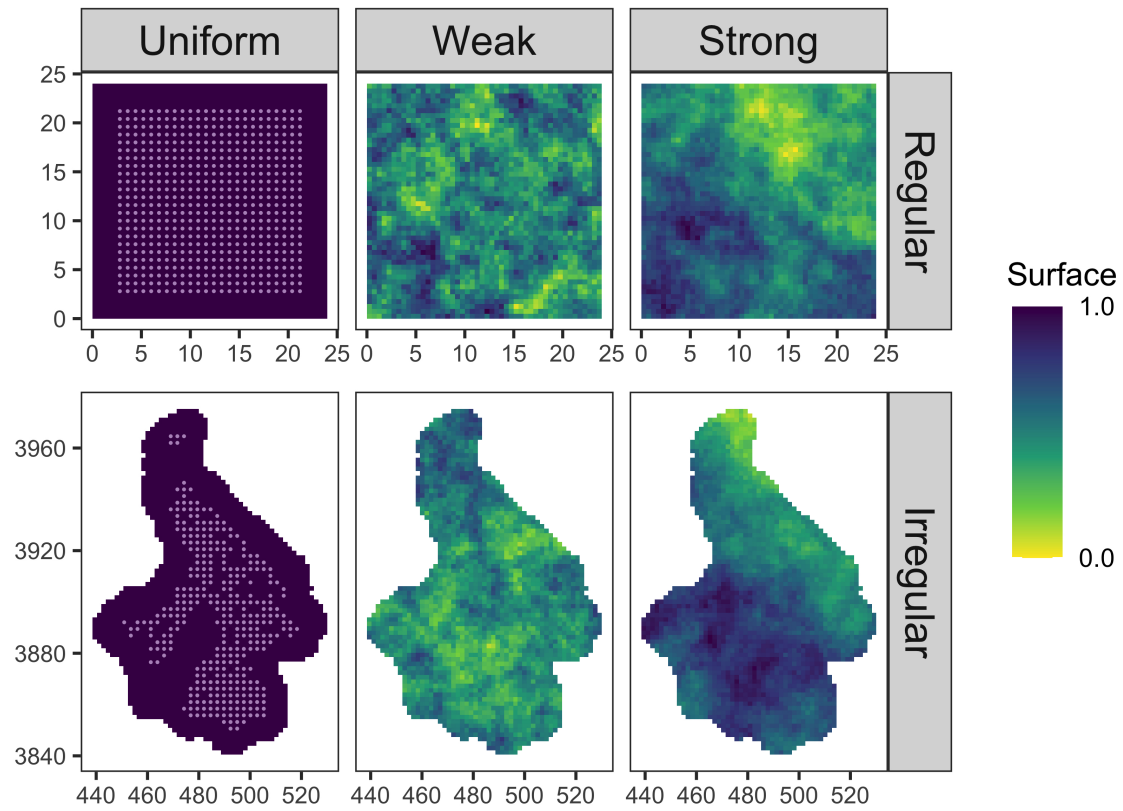


Figure 2

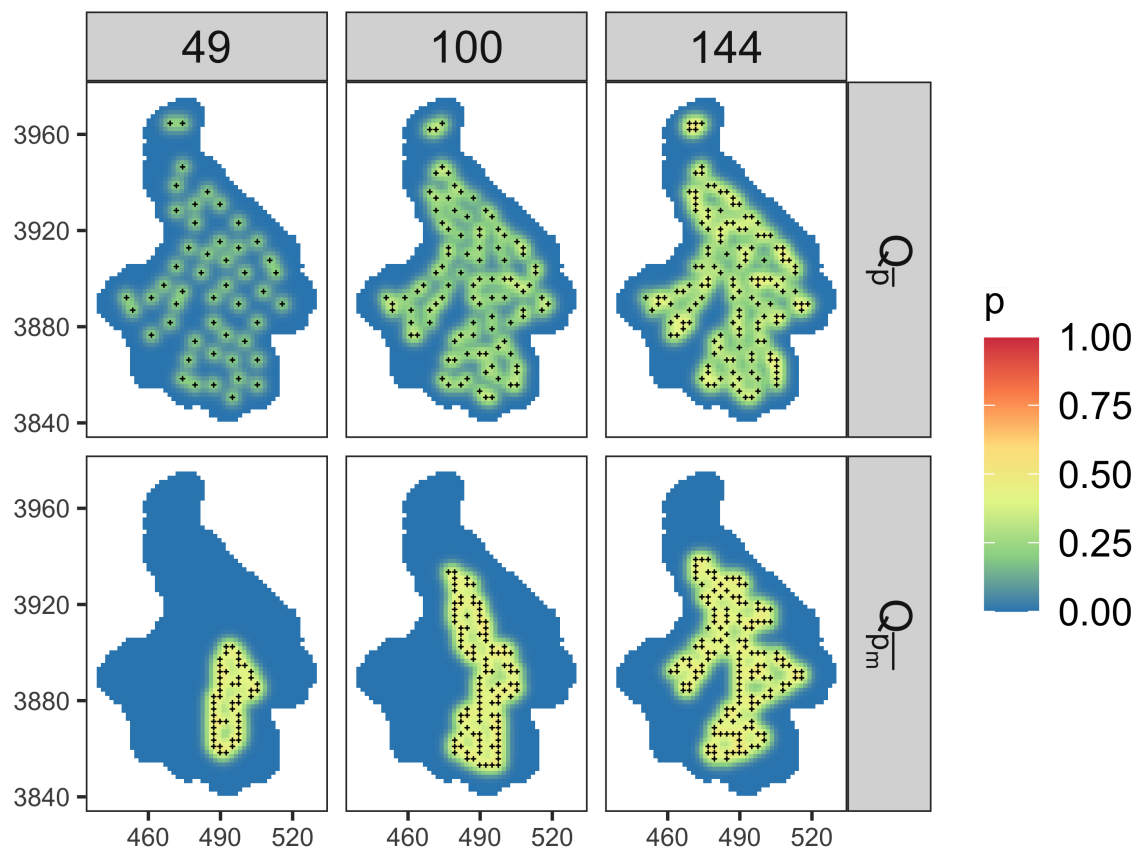


Figure 3

